

## Femtosecond near-field spectroscopy of a single GaAs quantum wire

T. Guenther, V. Emiliani,<sup>a)</sup> F. Intonti, C. Lienau, and T. Elsaesser

*Max-Born-Institut für Nichtlineare Optik und Kurzzeitspektroskopie, D-12489 Berlin, Germany*

R. Nötzel and K. H. Ploog

*Paul-Drude-Institut für Festkörperelektronik, D-10117 Berlin, Germany*

(Received 16 June 1999; accepted for publication 7 October 1999)

Quasi-two-color femtosecond pump and probe spectroscopy and near-field scanning optical microscopy are combined to study the carrier dynamics in single semiconductor nanostructures. In temporally, spectrally, and spatially resolved measurements with a time resolution of 200 fs and a spatial resolution of 200 nm, the nonlinear change in reflectivity of a single quantum wire is mapped in real space and time. The experiments show that carrier relaxation in a single quantum wire occurs on a 100 fs time scale at room temperature. © 1999 American Institute of Physics. [S0003-6951(99)05148-7]

Far-field femtosecond spectroscopic studies provide direct insight into the dephasing, scattering, and energy relaxation of free carriers and excitons in semiconductor nanostructures and have led to a detailed understanding of these processes.<sup>1</sup> In general, however, such studies give only indirect information on the ballistic and diffusive real-space transfer of photogenerated carriers or their trapping into low-dimensional nanostructures, as these processes involve the real-space motion of carriers on typical length scales of 10–1000 nm. Also, far-field resolution is often not sufficient to isolate the ultrafast response from a single nanostructure. Here, the combination of femtosecond spectroscopy with microscopy techniques giving subwavelength resolution, such as near-field scanning optical microscopy (NSOM),<sup>2,3</sup> offers new perspectives for a direct investigation of carrier dynamics on nanometer length scales. Yet only few experiments have been reported along this direction.<sup>4–6</sup> No applications to low-dimensional nanostructures such as quantum wires or dots have been reported so far. In this letter, we combine for the first time near-field microscopy and two-color femtosecond pump and probe spectroscopy to spectroscopically resolve the nonlinear optical response from a single (311) GaAs quantum wire (QWR) structure in real space and time.

Quantum wires with a thickness of up to 13 nm embedded in a 6 nm GaAs quantum well (QW) were grown on patterned GaAs (311)A substrates.<sup>7</sup> The total confinement energy in lateral (*y*) direction has a value of about 60 meV. The QWR/QW layer is clad between 50 nm Al<sub>0.5</sub>Ga<sub>0.5</sub>As barriers. The upper barrier is covered by a 20 nm GaAs cap layer [Fig. 1(a) (inset)].<sup>8–10</sup> At 300 K, the sample is characterized by intense photoluminescence (PL) [Fig. 1(a) (inset)] from both the QW (peaked at 1.52 eV) and QWR region (peaked at 1.46 eV).

Pump and probe pulses were derived from a 80 MHz Ti:sapphire oscillator; the laser output is split into a pump and a probe beam. Each beam travels through a separate prism setup for spectral shaping and precompensation of group velocity dispersion. Two optical configurations are used. In a near-field pump/near-field probe geometry, both pump and probe laser are transmitted through the same near-

field fiber probe. In a far-field pump/near-field probe geometry, only the probe pulse is sent through the fiber while the pump is focused down to 30 μm on the sample by a far-field (*f*=8 cm) lens. In both cases, the probe light reflected from the sample is collected in the far field, spatially and spectrally filtered and detected with a photodiode. Pump and probe beams are mechanically chopped at frequencies *f*<sub>1</sub> ≈ 1.2 kHz and *f*<sub>2</sub> = 1.77\**f*<sub>1</sub>, respectively and the photodiode signal is recorded at the sum frequency *f*<sub>1</sub>+*f*<sub>2</sub>. Aperture probes are made by chemically etching optical fibers.

First, far-field pump/near-field probe spectra were recorded in the QW region of the sample. The pump pulses (bandwidth 40 meV) are centered at the QW absorption resonance at 1.52 eV. The excitation density was about 3 × 10<sup>11</sup> cm<sup>-2</sup>. The pump induced change in reflectivity is sensed by tunable probe pulses of 11 meV bandwidth. In Fig. 1(a), the reflectivity change  $\Delta R/R_0(t_d) = (R(t_d) - R_0)/R_0$  for a time delay *t*<sub>d</sub> of 10 ps between pump and probe is plotted as a function of the probe energy *E*<sub>pr</sub> (*R*, *R*<sub>0</sub>: sample reflectivity with and without pump). For photon energies of the probe between 1.51 and 1.55 eV, the creation of electron-hole pairs results in an increase in reflectivity whereas a decrease of reflectivity is found for *E*<sub>pr</sub> < 1.51 eV. This spectrum shows a pronounced maximum at *E*<sub>pr</sub> = 1.515 eV and follows—for *E*<sub>pr</sub> ≥ 1.50 eV—the shape of the QW PL spectrum [inset of Fig. 1(a)]. These reflectivity changes rise within the time resolution of the experiment of 200 fs. For *E*<sub>pr</sub> ≥ 1.515 eV, the signal decays by carrier recombination on a nanosecond time scale.

Next, we present data taken in the range of the QWR resonance around 1.46 eV [cf. inset of Fig. 1(a)]. In this measurement, both pump and probe were transmitted through the fiber probe. Excitation at 1.51 eV generates carriers in high-lying QWR states, in the embedding QW and in the GaAs cap and substrate layers, and gives rise to a local change of reflectivity. This is evident from the image in Fig. 1(b) where the change of reflectivity at *E*<sub>pr</sub> = 1.45 eV and a delay time of 10 ps is plotted as a function of two spatial coordinates in the QW plane. The pronounced local change of reflectivity occurs along a line that coincides with the QWR position. This position is independently identified from shear-force topography images. The local reflectivity

<sup>a)</sup>Corresponding author: electronic mail: emiliani@mbi-berlin.de

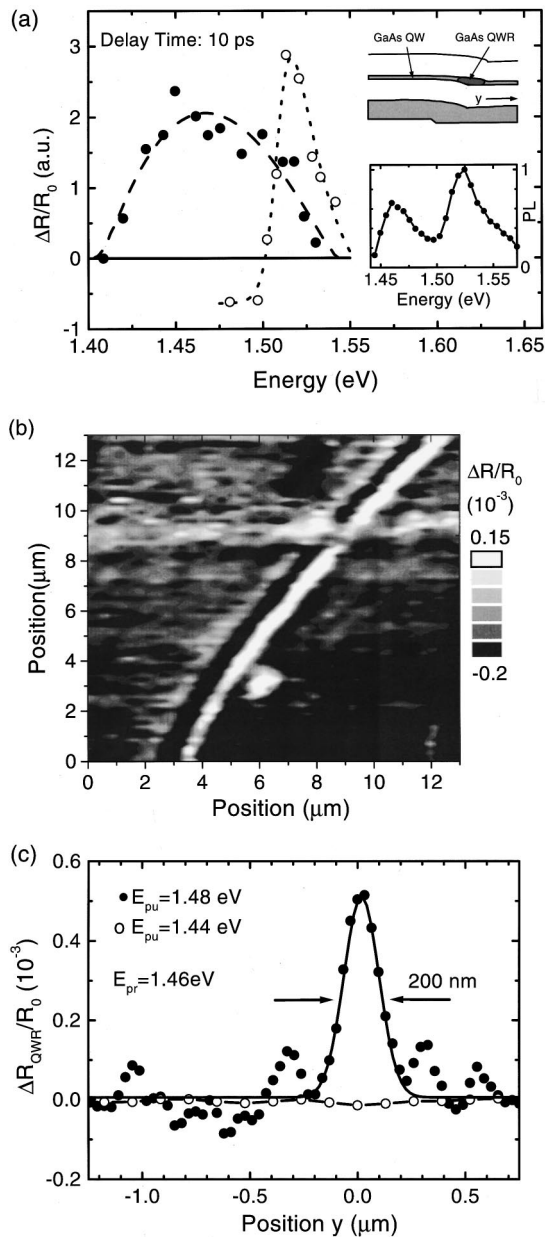


FIG. 1. (a) Probe wavelength dependence of the pump-induced quantum wire reflectivity change  $\Delta R_{QWR}(t_d=10\text{ ps})/R_0$  (closed circles) and of the reflectivity change in the mesa top region of the sample (open circles).  $E_{pu} = 1.52$  eV. Insets: schematic of the QWR sample and room temperature near-field photoluminescence spectrum. (b) Spatial map of the pump-induced reflectivity change  $\Delta R/R_0$  at a delay time  $t_d$  of 10 ps. The probe laser is set to 1.45 eV. (c) Spatial variation of  $\Delta R_{QWR}/R_0$  along a line perpendicular to the wire axis at a probe wavelength of  $E_{pr} = 1.46$  eV. Closed circles:  $E_{pu} = 1.48$  eV, open circles:  $E_{pu} = 1.44$  eV.

change is superimposed on a spatially slowly varying background signal which is due to the GaAs cap and substrate layers. The variation of the reflectivity change  $\Delta R_{QWR}/R_0 = [\Delta R(y=0) - \Delta R(|y| > 1\ \mu\text{m})]/R_0$  with probe energy  $E_{pr}$  is presented in Fig. 1(a) (solid circles) for a delay of 10 ps [ $\Delta R(|y| > 1\ \mu\text{m})$ : background signal]. The line shape resembles the shape of the QWR PLE spectrum.<sup>10</sup>

In Fig. 1(c), the quantity  $\Delta R_{QWR}/R_0$  is plotted along the  $y$  direction, i.e., perpendicular to the QWR axis ( $y=0$ : QWR position), for two different pump energies  $E_{pu}$ . The local reflectivity peak is measured with a spatial resolution of 200 nm, partially limited by the distance between QWR and

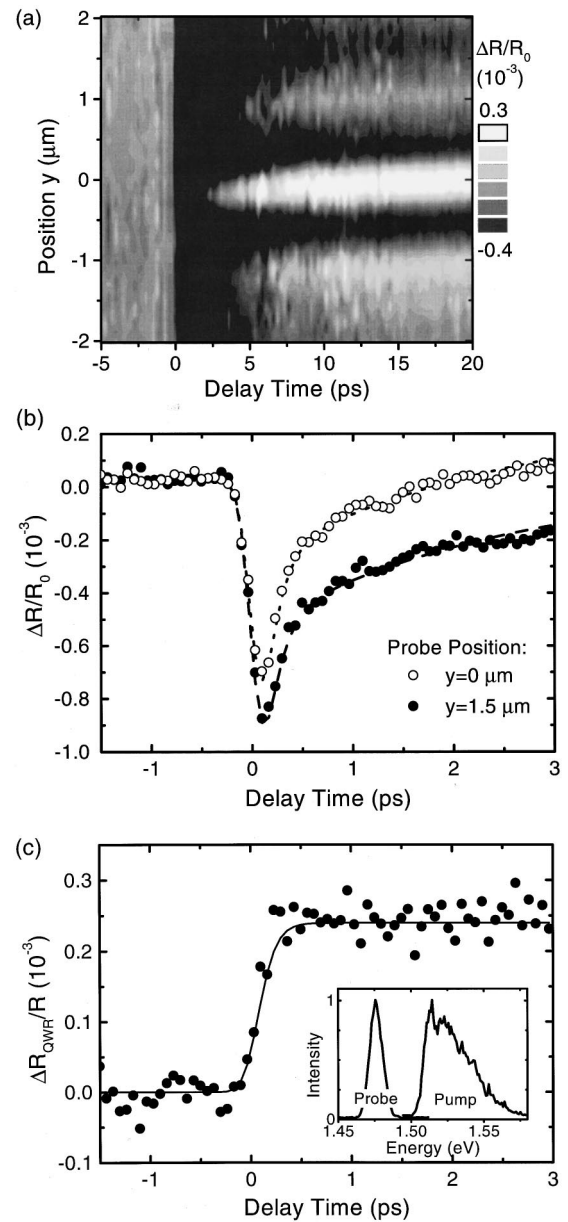


FIG. 2. (a) Pump-induced reflectivity change  $\Delta R/R_0$  as a function of tip position along the  $y$  axis, perpendicular to the quantum wire axis, and as a function of delay time  $t_d$ .  $E_{pu} = 1.51$  eV,  $E_{pr} = 1.475$  eV. (b) Temporal variation of  $\Delta R/R_0$  at fixed spatial probe positions of  $y=0$  (QWR position, open circles) and on the mesa top part at  $y=1.5\ \mu\text{m}$  ( $\Delta R_{QWR}(t_d)/R_0 = [\Delta R(y=0, t_d) - \Delta R(y=1.5\ \mu\text{m}, t_d)]/R_0$ ). Inset: spectra of pump and probe laser.

sample surface of about 70 nm. For excitation at 1.44 eV [Fig. 1(c), open circles] where the QWR absorption is negligible, the reflectivity change vanishes completely. These results demonstrate that the local reflectivity change  $\Delta R_{QWR}$  is due to carriers in the QWR and depends on their transient distribution and overall concentration.

The time evolution of  $\Delta R_{QWR}(t_d)$  gives insight into carrier dynamics in the QWR. We investigated the relaxation of energetic carriers generated with a 50 fs far-field pump pulse at 1.51 eV. The carrier dynamics in the QWR are probed by measuring  $\Delta R_{QWR}(t_d)$  with a probe pulses at 1.475 eV, i.e., near the QWR resonance, which are transmitted through the near-field fiber probe. In Fig. 2(a), the reflectivity change  $\Delta R(y, t_d)$  is plotted as a function of the lateral coordinate  $y$

and the delay time  $t_d$ . On both sides of the QWR, a spatially homogenous transient reflectivity decrease is observed that decays on a time scale of a few picoseconds. This is shown in Fig. 2(b) (solid circles) where the time evolution of  $\Delta R(y=1.5 \mu\text{m})$  is plotted versus delay time. In contrast, a decrease of reflectivity with smaller amplitude occurs at the QWR position  $y=0$  [open circles in Fig. 2(b)]. A fast change of reflectivity, on a 1 ps time scale, is present in both curves, and reflects the trapping of carriers into surface states.<sup>11</sup> The QWR contribution  $\Delta R_{\text{QWR}}(t_d)/R_0$  to the overall reflectivity change is extracted by taking the difference of the two transients in Fig. 2(b). The time evolution of  $\Delta R_{\text{QWR}}(t_d)/R_0$  plotted in Fig. 2(c) shows an ultrafast rise within 200 fs, the time resolution of the experiment. Similar transients are measured with pump pulses attenuated by a factor of 3.

The reflectivity spectra depend sensitively on details of the layer structure.<sup>12</sup> To interpret our experiments we performed an analysis of the pulse propagation through our multilayer nanostructure. The structure consists of the GaAs cap layer, the GaAs QW in which the QWR is embedded, the GaAs substrate and—in-between—the AlGaAs barriers. For photon energies  $E_{\text{pu}} < 1.44 \text{ eV}$ , only the cap layer and the substrate are excited, for  $1.44 \text{ eV} < E_{\text{pu}} < 1.50 \text{ eV}$  those layers and the QWR. For higher photon energies, carriers are also created in the QW. Carrier generation leads to a modification of the optical susceptibility  $\chi(\omega, n_{\text{ex}})$  of each layer with carrier density  $n_{\text{ex}}$ . This results in a change of reflectivity measured at the different probe wavelengths. A numerical simulation of these changes assuming thermalized carrier distributions for both electrons and holes was performed by using the numerical matrix inversion method.<sup>13</sup> The assumption of thermalized distributions is reasonably justified, as our time resolution is less than the sub-100 fs dephasing and thermalization times of free carriers in two-dimensional (2D) quantum wells at room temperature.<sup>14</sup> The model accounts quantitatively for the influence of phase-space filling, screened Coulomb interaction, here treated in a static approximation, and band-gap renormalization on  $\chi(\omega, n_{\text{ex}})$ . It gives absolute values for the density dependent absorption coefficient  $\alpha(\omega, n_{\text{ex}})$  and refractive index  $n_r(\omega, n_{\text{ex}})$  of each layer. A transfer matrix formalism is then used to derive the reflectivity  $R(\omega, n_{\text{ex}})$  and the carrier-induced change in reflectivity  $\Delta R(\omega, n_{\text{ex}}) = R(\omega, n_{\text{ex}}) - R(\omega, 0)$  for the multilayer structure.

This analysis suggests the following interpretation: For  $E_{\text{pu}} > 1.5 \text{ eV}$ , excitation of the QW leads to a decrease of interband absorption around the QW absorption resonance at  $E_{\text{pr}} = 1.52 \text{ eV}$ , i.e., of the imaginary part of the susceptibility. This results in an increase in reflectivity [open circles in Fig. 1(a)] with a spectral dependence close to the QW PL spectrum (inset). At probe energies  $E_{\text{pr}} < 1.5 \text{ eV}$ , the reflectivity change is dominated by the cap layer and has the opposite sign. The change in sign occurs because the cap layer signal is most sensitive to the change in refractive index, i.e., the real part of the susceptibility.

Now we consider the signals measured with the fiber probe at the QWR. Here, the additional contribution due to carriers in the QWR results in a smaller amplitude of the change of reflectivity [open circles in Fig. 2(b)]. This contribution is described by the quantity  $\Delta R_{\text{QWR}}/R_0 = [\Delta R(y$

$= 0) - \Delta R(|y| > 1 \mu\text{m})]/R_0$ . The spectrum of  $\Delta R_{\text{QWR}}/R_0$  in Fig. 1(a) resembles the PLE spectrum of the QWR. As for the QW, the QWR reflectivity change results from the carrier induced bleaching of the QWR absorption and is mainly sensitive to the imaginary part of the susceptibility, thus having a positive sign.

The QWR signal  $\Delta R_{\text{QWR}}$  is sensitive to the concentration and energy distribution of carriers in the QWR. For  $E_{\text{pu}} = 1.51 \text{ eV}$  [Figs. 2(b) and 2(c)], carriers are excited to both high lying QWR states and into the surrounding QW. Probing at  $E_{\text{pr}} = 1.46 \text{ eV}$ , i.e., at the bottom of the QWR, one observes a rise of  $\Delta R_{\text{QWR}}$  within the time resolution of 200 fs and a constant amplitude at later times. There are two mechanisms contributing to this behavior, screening of the QWR absorption resonance by the optically injected carriers and bandfilling due to a carrier population in the low-lying states of the QWR. Both effects are expected to be present.<sup>15</sup> The first mechanism rises with the optically generated carrier concentration, i.e., follows instantaneously the time integral of the pump pulse. In contrast, the second mechanism requires carrier redistribution from optically excited high lying states to the bottom of the QWR. The absence of any slower dynamics on the transient in Fig. 2(c) suggests that this redistribution process occurs within the first 200 fs. Both carrier-carrier and carrier-LO phonon scattering contribute to this fast relaxation. Furthermore, the constant signal at later times shows that there is no significant proliferation of carriers from the embedding QW into the QWR.

In conclusion, we have demonstrated, for the first time, the potential of femtosecond near-field spectroscopy for directly imaging the carrier dynamics in a single semiconductor nanostructure and have resolved the ultrafast relaxation of carriers into a single QWR on a 100 fs time scale at room temperature.

V.E. gratefully acknowledges a Marie-Curie fellowship (ERB4001GT975127).

<sup>1</sup>For a recent overview, see J. Shah, *Ultrafast Spectroscopy of Semiconductors and Semiconductor Nanostructures*, 2nd ed. (Springer, Berlin, 1999).

<sup>2</sup>D. W. Pohl, W. Denk, and M. Lanz, *Appl. Phys. Lett.* **44**, 651 (1984).

<sup>3</sup>E. Betzig and J. K. Trautman, *Science* **257**, 189 (1992).

<sup>4</sup>J. B. Stark, U. Mohideen, E. Betzig, and R. E. Slusher, in *Ultrafast Phenomena IX*, Springer Series in Chemical Physics (Springer, Berlin, 1996), p. 349.

<sup>5</sup>J. Levy, V. Nikitin, J. M. Kikkawa, A. Cohen, N. Samartha, R. Garcia, and D. D. Awschalom, *Phys. Rev. Lett.* **76**, 1948 (1996).

<sup>6</sup>B. A. Nechay, U. Siegner, F. Morier-Genoud, A. Schertel, and U. Keller, *Appl. Phys. Lett.* **74**, 61 (1999).

<sup>7</sup>R. Nötzel, M. Ramsteiner, J. Menniger, A. Trampert, H.-P. Schönherr, L. Däweritz, and K. H. Ploog, *Jpn. J. Appl. Phys., Part 2* **35**, L297 (1996).

<sup>8</sup>A. Richter, G. Behme, M. Süptitz, Ch. Lienau, T. Elsaesser, M. Ramsteiner, R. Nötzel, and K. H. Ploog, *Phys. Rev. Lett.* **79**, 2145 (1997).

<sup>9</sup>Ch. Lienau, A. Richter, G. Behme, M. Süptitz, D. Heinrich, T. Elsaesser, M. Ramsteiner, R. Nötzel, and K. H. Ploog, *Phys. Rev. B* **58**, 2045 (1998).

<sup>10</sup>A. Richter, M. Süptitz, D. Heinrich, Ch. Lienau, T. Elsaesser, M. Ramsteiner, R. Nötzel, and K. H. Ploog, *Appl. Phys. Lett.* **73**, 2176 (1998).

<sup>11</sup>J. J. Baumberg, D. A. Williams, and K. Köhler, *Phys. Rev. Lett.* **78**, 3358 (1997).

<sup>12</sup>M. Gurioli, S. Piantelli, M. Colocci, and S. Franchi, *Appl. Phys. Lett.* **74**, 3365 (1999).

<sup>13</sup>S. Schmitt-Rink, C. Ell, and H. Haug, *Phys. Rev. B* **33**, 1183 (1986).

<sup>14</sup>D. S. Kim, J. Shah, J. E. Cunningham, T. C. Damen, W. Schäfer, M. Hartmann, and S. Schmitt-Rink, *Phys. Rev. Lett.* **68**, 1006 (1992).

<sup>15</sup>H. Haug and S. W. Koch, *Quantum Theory of the Optical and Electronic Properties of Semiconductors* (World Scientific, Singapore, 1993).